

UC Riverside

UC Riverside Previously Published Works

Title

Synthesis of New S-S and C-C Bonds by Photoinitiated Radical Recombination Reactions in the Gas Phase.

Permalink

<https://escholarship.org/uc/item/9rp4t1td>

Authors

Talbert, Lance E
Zhang, Xing
Hendricks, Nathan
et al.

Publication Date

2019-07-01

DOI

10.1016/j.ijms.2019.04.002

Peer reviewed

Synthesis of New S-S and C-C Bonds by Photoinitiated Radical Recombination Reactions in the Gas Phase

Lance E. Talbert, Xing Zhang, Nathan Hendricks, Arman Alizadeh and Ryan R. Julian*

Department of Chemistry, University of California, Riverside, 501 Big Springs Road,
Riverside, CA 92521, USA, (951) 827- 3959

* ryan.julian@ucr.edu

Abstract

Photoinitiated radical chemistry has proven to be useful for breaking covalent bonds within many biomolecules in the gas phase. Herein, we demonstrate that radical chemistry is useful for bond synthesis in the gas phase. Single peptides containing two cysteine residues capped with propylmercaptan (PM) often form disulfide bonds following ultraviolet excitation at 266 nm and loss of both PM groups. Similarly, noncovalently bound peptide pairs where each peptide contains a single cysteine residue can be induced to form disulfide bonds. Comparison with disulfide bound species sampled directly from solution yields identical collisional activation spectra, suggesting that native disulfide bonds have been recapitulated in the gas phase syntheses. Another approach utilizing radical chemistry for covalent bond synthesis involves creation of a reactive diradical that can first abstract hydrogen from a target peptide, creating a new radical site, and then recombine the second radical with the new radical to form a covalent bond. This chemistry is illustrated with 2-(hydroxymethyl-3,5-diiodobenzoate)-18-crown-6 ether, which attaches noncovalently to protonated primary amines in peptides and proteins. Following photoactivation and crosslinking, the site of noncovalent adduct attachment can frequently be determined. The ramifications of these observations on peptide structure and noncovalent attachment of 18-crown-6-based molecules is discussed.

Introduction

Manipulation of ions within mass spectrometers is more often used to break bonds than to make them. However, the synthesis of new bonds affords extraction of novel information such as structural relationships or relative reactivity, which has motivated a limited number of studies. For example, irradiation of photoleucine can lead to covalent coupling of peptides by insertion of reactive carbenes.¹ Carbenes can also be generated by collisional activation of diazo groups, even when molecules to be coupled are only held together by noncovalent bonds.² Carbene chemistry is advantageous in that covalent links are easily formed by insertion to a large variety of bonds, but at the same time such crosslinks are dictated primarily by proximity and afford poor chemical selectivity. Covalent bonds have also been synthesized by a variety of ion/ion reactions pioneered by the McLuckey lab that rely on reactive functional groups and do afford selectivity.³⁻⁵ New bonds can also be created by accessing excited state reactivity, as demonstrated in experiments where vacuum ultraviolet light led to condensation reactions between peptide fragments.⁶ Taken together, these studies have revealed that covalent bond formation is possible in the gas phase if reactive species can be brought into sufficiently close proximity for enough time to allow the coupling to proceed.

Radicals are another highly reactive group with the potential to form covalent bonds. Both the recombination of two radicals or insertion of a radical into a suitable bond followed by elimination of a different radical can lead to the formation of new covalent linkages. Indeed, radical recombination of separately generated radical species was previously used to probe the conformational states of polyproline peptides.⁷ Similar to photoleucine, chemistries are available for the highly specific creation of radicals by photoactivation of ultraviolet (UV) labile groups.^{8,9} Both open shell carbon and sulfur atoms can be created at atomically precise locations in this fashion with little additional heating of the remaining molecule.¹⁰ Radicals can also be generated by collisional activation, which can lead to intramolecular bond formation reactions useful for examining covalent architecture such as disulfide bonds.¹¹ However, once again in the majority

of cases, radical chemistry is utilized to modulate dissociation when applied to biomolecular study rather than to initiate bond formation.¹²⁻

Herein we demonstrate that radicals can be used to efficiently create covalent bonds. New S-S bonds that recapitulate native disulfide links can be generated in highly efficient gas phase reactions in both intramolecular and intermolecular systems. New C-C bonds can be created from diradical, noncovalently bound species, allowing for the location of noncovalent adducts to be investigated. The details and potential applications of these reactions are discussed.

Experimental Methods

Materials

Peptides RGDC, VTCG, PHCKRM, YGLSKGCFGLKLD RIGSMSGLGC, and SPKTM RDSGCFGRRLDRIGSLSGLCNVLRRY were purchased from American Peptide Company (Sunnyvale, CA). SLRRSSCFGGR and CQDSETRTFY were purchased from Abbiotec (San Diego, CA) and CDPGYIGSR was purchased from Apexbio. Ammonium bicarbonate was purchased from Avantor (Center Valley, PA). Dithiothreitol was purchased from Arcos Organics (Geel, Belgium). Dimethyl sulfoxide (DMSO) were purchased from Sigma-Aldrich (St. Louis, MO). Trifluoroacetic acid (TFA) and N,N'-Dicyclohexylcarbodiimide was purchased from Alfa Aesar (Haverhill, MA). Acetonitrile (ACN), methanol and 1,4 dioxane were purchased from Fisher Scientific (Waltham, MA). 2-hydroxymethyl-18-crown-6 ether was purchased from TCI America (Portland, OR) and 3,5-diiodobenzoic acid was purchased commercially. Water was purified by Millipore Direct-Q (Millipore, Billerica, MA). A MacroTrap holder and MacroTrap consisting of polymeric reversed-phase packing material were purchased from Michrom Bioresources, Inc. (Auburn, CA).

Peptide and Protein Derivatization with Propyl mercaptan

Disulfide containing peptides were reduced as follows: 10 μ L of a 1 mM peptide stock was diluted in 25 μ L of 50 mM ammonium bicarbonate. To this solution, 1.5 μ L of dithiothreitol (DTT)

was added and the resulting solution was incubated in the dark at 37 °C for 1 hour. To remove salt from the mixture, the peptide was purified by MacroTrap and eluted in 0.1%TFA in 2%:98% H₂O:ACN and lyophilized to a powder.

The lyophilized powder was dissolved in 10 µL of water. Modification of the free thiols was carried out by adding 10 µL of dimethyl sulfoxide and 1.5 µL of propyl mercaptan to the peptide solution. This mixture was placed in a 37 °C water bath overnight. The peptide was subsequently cleaned by Macrotrap and eluted in 0.1%TFA in 2%:98% H₂O:ACN, lyophilized to a powder and dissolved in 50:50 H₂O:MeOH in 0.1% formic acid for a final concentration of 10 µM for MS analysis.

For the intermolecular disulfide formation experiments, peptides containing a single cysteine were modified with propyl mercaptan as described above. In order to encourage peptide interaction, peptides were mixed together to obtain final concentrations of roughly 100-150 µM for MS analysis.

Synthesis of 2-(hydroxymethyl-3,5-diiodobenzoate)-18-crown-6 ether (BC)

The synthesis of 2-(hydroxymethyl-3,5-diiodobenzoate)-18-crown-6 ether was carried out using a protocol previously described.⁸ Briefly, 0.5 mmol DCC was dissolved in 5 mL of dioxane and added to a round bottom flask containing 0.50 mmol of 3,5-diiodobenzoic acid and 0.50 mmol of 2-hydroxymethyl-18-crown-6 ether. The mixture was left to react for 12 hours and gravity filtration was used to remove the crystalline hair-like precipitate.

Noncovalent Adduct of Synthetic Crown (BC)

Peptides and proteins were dissolved in a mixture of 50:50 H₂O:MeOH in 0.1% formic acid to obtain a final concentration of 10 µM. The synthetic crown BC was added to each of the solutions in a ratio of 1:4 (BC:tertiary amine). The number of BC noncovalent adducts observed varied for each sample.

Photodissociation of Peptides and Proteins

An LTQ linear ion trap mass spectrometer (Fisher Scientific, Waltham, MA) with a standard ESI source was utilized mass analysis. A quartz window was installed on the back plate of the LTQ for transmission of laser pulses from a flash-lamp pumped Nd:YAG Minilite laser (Continuum, Santa Clara, CA). For all experiments except those with ubiquitin, a single pulse of fourth harmonic (266 nm) 4 mJ light was triggered during the MS² activation step. For the ubiquitin+BC experiments, four pulses were triggered during the MS² activation step. Peptides were sprayed at the concentrations stated above at 3 μ L/min with electrospray voltage of 3.25 kV and a capillary inlet temperature set to 215 °C.

Results and Discussion

Intramolecular Disulfide Formation. Disulfide bonds are commonly found within peptides and proteins.¹⁸ In proteins, such bonds help define tertiary and quaternary structure. In peptides, disulfide bonds are common in venoms and toxins where the crosslink not only serves to define structure and promote toxicity, but also helps prevent deactivation by proteolysis.^{19,20} Peptides in aqueous solution that contain cysteine in the free thiol state can spontaneously form disulfides in the presence of oxygen, particularly if the pH is above 8.²¹ Similar chemistry does not occur in the gas phase because solvent is not available to facilitate deprotonation of the thiol. Previous work has demonstrated that disulfide bonds can be selectively cleaved by UV photons, yielding homolytic cleavage of the S-S bond and two sulfur radicals.^{9,22} In addition to native disulfide bond cleavage, cysteine residues modified with propyl mercaptan (PM) are also susceptible to homolytic fragmentation by either direct photon absorption or via energy transfer.^{23,24} This type of fragmentation is demonstrated in Fig. 1a for the 3+ charge state of porcine brain natriuretic peptide (BNP) 1-32 that had been reduced and then modified with PM at both cysteine residues (native sequence = SPKTMRDSGC FGRRLDRIGS LSGLGCNVLR RY, where Cys9 and Cys26 form a disulfide bond). The loss of one and two PMs yields the most abundant products in Fig. 1a. The double PM loss creates a biradical species that could, in

theory, recombine to form a disulfide by the pathway shown in Scheme 1a. Additional pathways are available following a single PM loss, which can yield a sulfur radical at either cysteine residue specifically or at a combination of both sites. Subsequent collisional activation of this product cannot distinguish between these options because loss of the second PM radical represents the primary product, as shown in Fig. 1b. This suggests that regardless of which sulfur radical is initially created, selective attack to displace the second PM and reform the native disulfide bond is the most favored outcome. This mechanism is shown in Scheme 1b.

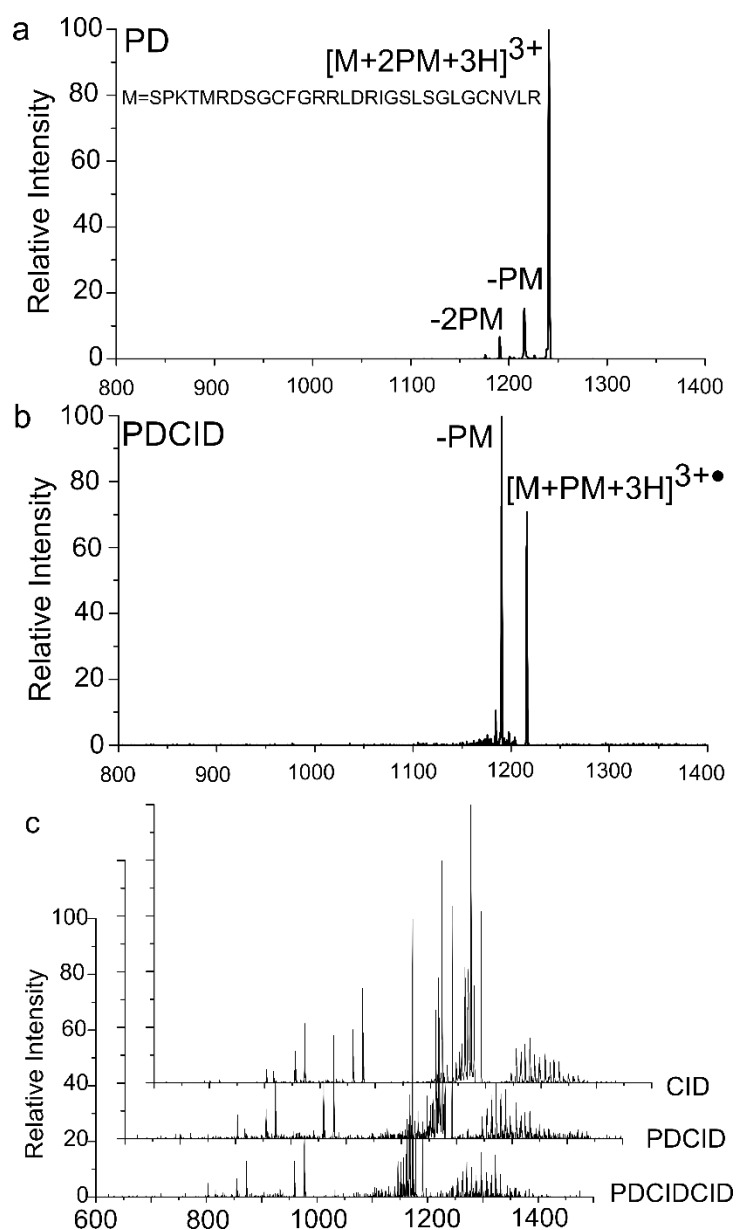
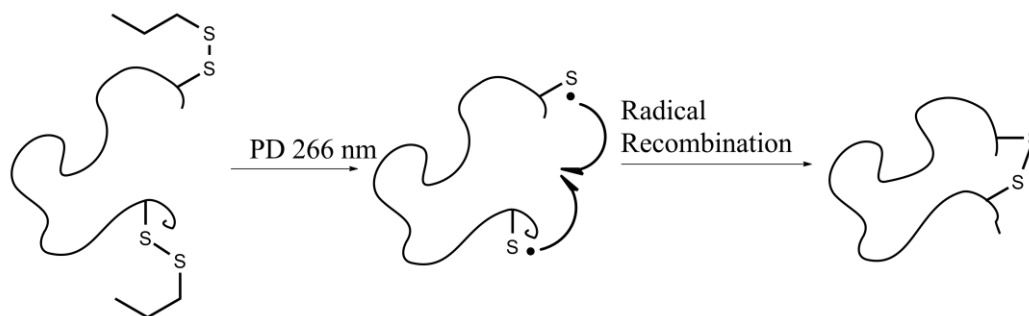
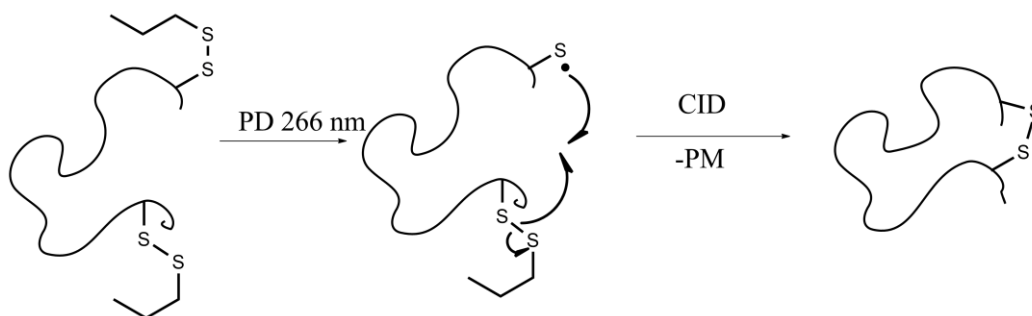


Figure 1: a) Photodissociation of the +3 charge state of BNP yields loss of one and two PM modifications. b) CID of the single PM loss leads to loss of the second PM. c) Stacked mass spectra comparing canonical peptide (CID) to disulfide generated by double loss of PM (PDCID) observed in (a) and sequential loss of two PM observed in (b). All three spectra are very similar, suggesting the same disulfide is activated in each case.

a) Biradical Recombination



b) Sequential Radical Attack



Scheme 1: a) Biradical species can recombine to directly form a disulfide bond. b) A single thiol radical can attack a nearby disulfide, leading exchange and loss of a different thiol radical.

To confirm disulfide bond formation, fragmentation of the product ions can be compared with that of the native disulfide electrosprayed directly from solution. Fragmentation data for both disulfides generated in the gas phase are compared with the native results in the stacked plot in Fig. 1c. The bona fide disulfide bound peptide yields a complex spectrum with many product ions, consistent with its cyclic nature that requires fracture of multiple bonds to observe

fragmentation within the ring (Fig. 1c, top). The lower two spectra derived from gas phase syntheses are very similar. The probability for reproducing such complex spectra from different molecular structures is low, suggesting that disulfide bond formation occurred for both the simultaneous and sequential double PM losses. The selectivity of the sequential attack (Scheme 1b) can be rationalized in terms of the relative reactivity of the sulfur radical initially generated by photodissociation. Sulfur radicals are stable relative to most positions within a peptide, making radical migration to most locations energetically uphill and unfavorable.^{25,26} However, attack of another disulfide bond creates an equally stable radical, which is neutral from a thermodynamic perspective. Radical attack of disulfides in related systems has been shown to be energetically favorable and occur with relatively low activation energies.^{11,27,28} The results illustrate that the two sulfur moieties encounter each other prior to the addition of sufficient energy to enable uphill radical migration or another dissociation pathway.

Similar experiments were conducted with Type C natriuretic peptide (CNP) with sequence YGLSKGCFGL KLDRIGSMMSG LGC that contains a native disulfide bond between Cys7 and Cys23. After reduction and modification with two equivalents of PM, photoactivation of the 4+ ion at 266 nm yields the spectrum shown in Fig. 2a. Interestingly, the loss of two PM is the most abundant loss, contrasting the results from BNP in Fig. 1a. The double loss again results in formation of a disulfide bond and a subsequent activation spectrum indistinguishable from the native peptide, see insets in Fig. 2a. Collisional activation of the single PM loss, however, does not yield primarily loss of a second PM as shown in Fig. 2b. Loss of the second PM is the most abundant product, but many additional fragments are noted, including backbone dissociation where the PM modification has been retained as highlighted in the inset of Fig. 2b. These fragments reveal that the initial PM was lost from both cysteine residues, though loss was more favorable from Cys7. This may be due to the closer proximity of Cys7 to Tyr1, which could enhance disulfide bond cleavage by energy transfer. In any case, there appear to be two structure populations for CNP, one where the two cysteine residues can easily interact and form

a disulfide bond, and a second structure where this is prohibited by significant energy barriers. The additional charge (4+ versus 3+) relative to the BNP should lead to greater Coulomb repulsion and may structural flexibility. Subsequent activation of the –PM product peak from Fig. 2b leads to a fragmentation spectrum similar to that of the native disulfide peptide (see Fig. 2c), although the presence of additional peaks may indicate a more complicated cross-linked product was created as well.

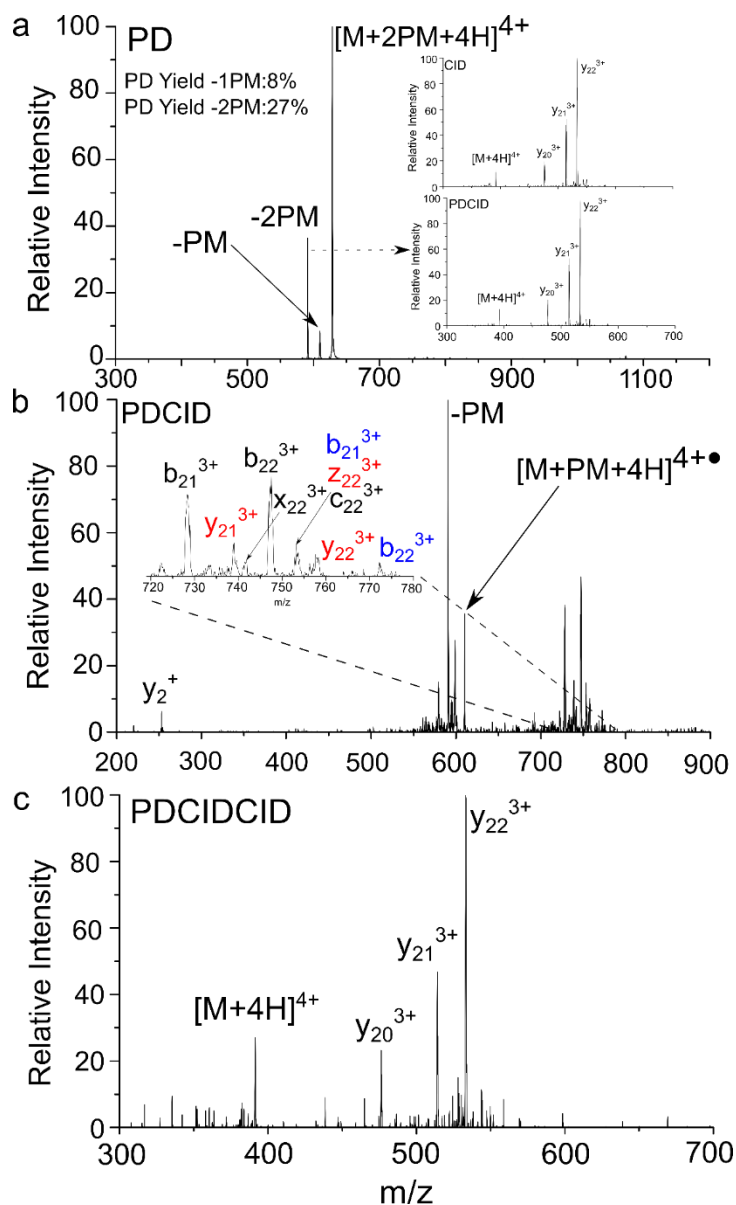


Figure 2: a) Photodissociation of the +4 charge state of YGLSKGC₇FGL KLDRI²³MSG LGC₂₃ yields primarily loss of both PM modifications. The insets compare collisional activation of solution (top) and gas phase (bottom) synthesized disulfides. b) CID activation of the single PM loss from the PD step. Blue labeled fragments indicate retention of PM at Cys23, black fragments indicate retention of PM at Cys7, and red fragments are ambiguous to the location of the PM modification. c) CID activation of the sequential PM loss observed in b.

Intermolecular Disulfide Formation. Disulfide bonds can also connect two different peptide strands, as occurs in the well-known case of insulin. To evaluate whether it is possible to synthesize such a bond in the gas phase, we electrosprayed a solution containing two peptides, each with a single cysteine (RGDC and CQDSE⁷TRTFY). Under gentle electrospray, a noncovalent complex comprised of these two peptides can be observed and photoactivation yields the spectrum shown in Fig. 3a. Interestingly, the weak noncovalent bonds holding the complex together are not broken, but losses of one and two PMs are noted with the double loss being significantly favored. Subsequent activation of the -2PM product yields a spectrum nearly identical to collisional activation of the disulfide bound pair directly electrosprayed into the mass spectrometer (Fig. 3b and 3c). Given the low absorption of disulfide bonds, it is highly unlikely that the majority of the double -PM loss is generated by two separate photodissociation events. More likely, the loss of either PM individually enables attack at the remaining PM site and subsequent loss of the second PM to form the disulfide bond. Collisional activation of the single PM loss leads primarily to separation of the two peptides, suggesting the existence of a conformation that is unable to bring both cysteine residues into close proximity prior to reaching the noncovalent dissociation threshold.

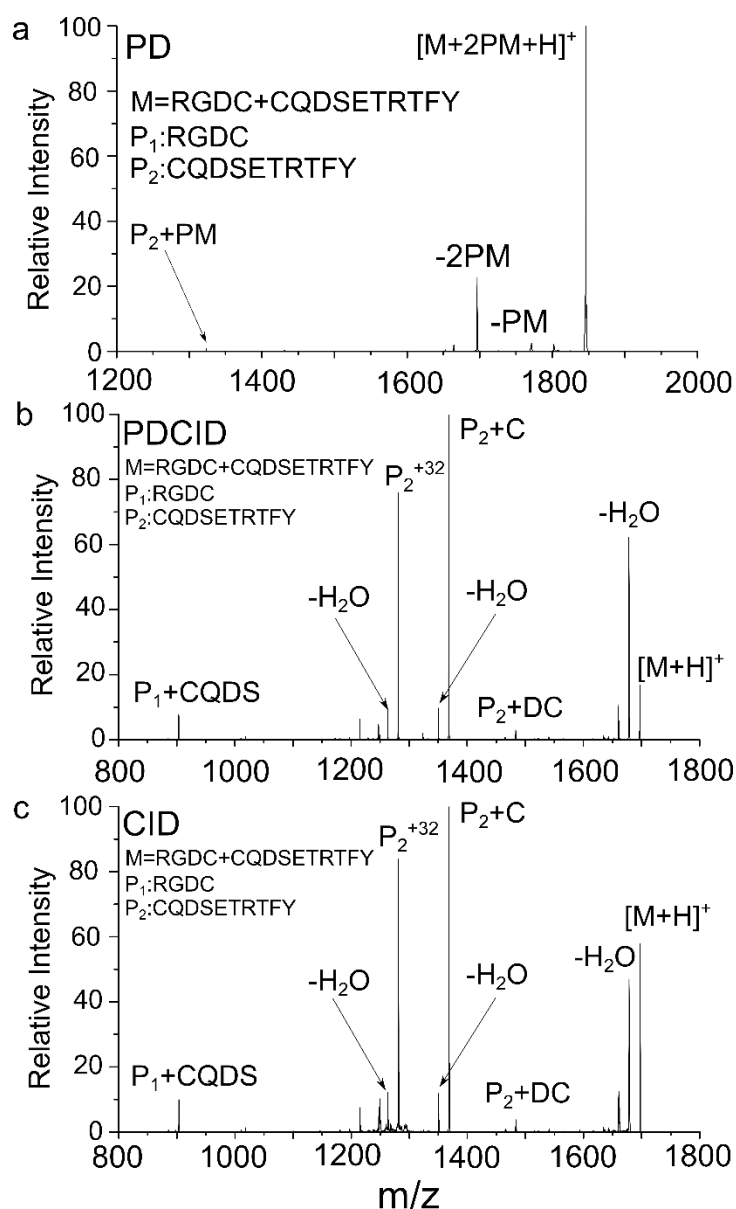


Figure 3: a) PD of the two noncovalent peptides RGDC and CQDSETRTFY each modified with PM. b) Subsequent CID activation of the loss of 2PM modifications from PD. c) CID fragmentation of the liquid phase formed disulfide linkage. P_1+CQDS refers to the peptide RGDC linked to the CQDS portion of P_2 , while P_2+^{32} refers to CQDSETRTFY with an additional 32 Da mass corresponding to the sulfur from RGDC. $-H_2O$ refers to losses from the labeled peaks immediately to the right.

The results in Fig. 3 clearly demonstrate it is possible to form disulfide bonds between noncovalently bound peptide pairs. However, to better evaluate the likelihood for such chemistry, a variety of peptide pairs were examined and the results are summarized in Table 1. The ratio of single to double PM loss varies by peptide pair, most likely due to structural differences that influence the ability of the two PM groups to interact with each other. However, in every case the -2PM loss is observed, and the subsequent collisional activation spectra are close matches to CID spectra of the native disulfide. Although it is interesting that disulfide bonds can be synthesized in the gas phase, the implications of these results are also important in a larger context. The facility of so many peptides and peptide pairs to form disulfide bonds suggests that peptide structures are either 1) highly flexible in the gas phase, allowing cysteine residues to ‘find’ each other, or 2) composed of highly heterogeneous mixtures of structures where some fraction of conformations contain cysteine residues in close proximity, or 3) some combination of both possibilities. Activation of the single PM loss products offers some insight into the matter. The sequential PM losses listed in Table 1 are not uniformly abundant, implying that high flexibility is certainly not a uniform property of noncovalent peptide dimers. Inherent within the ability to explore structural space is the strength of the noncovalent interactions binding the two peptides together, which likely varies significantly depending on the nature of the peptides. The data are consistent with a heterogeneous population of many structures, some of which contain cysteine residues in close enough proximity to form a disulfide bond following minimal activation.

Table 1: Peptide pairs and modifiers examined for disulfide formation

Peptide Pair	Double PM Loss (%)	Single PM Loss (%)	Sequential PM Loss (%)
RGDC+CQDSETRTFY (2PM)	18	2	7
CQDSETRTFY+SLRRSSCFGGR (2PM)	19	4	16

RGDC+CDPGYIGSR (2PM)	24	5	17
RGDC+SLRRSSCFGGR (2PM)	6	10	32
RGDC+PHCKRM (2PM)	9	9	17

Diradical Crosslinking. Previous work has demonstrated that covalent bonds can be formed in the gas phase by recombination of biradical species (where the two radicals are independent of each other).⁷ Another possibility can be envisioned starting with a diradical, where the two radicals are equivalent and contained on the same functional group. 2-(hydroxymethyl-3,5-diiodobenzoate)-18-crown-6 ether (BC) contains two C-I bonds which are photocleavable at 266 nm, affording a facile route to generate a diradical. Figure 4a shows the photoactivation of the peptide RGYALG noncovalently linked to BC. Dissociation of a single C-I bond is the major fragmentation pathway, yielding a single radical. Subsequent CID activation of the radical complex is shown in Figure 4b. As expected, collisional activation leads to migration of the radical to the peptide, loss of the noncovalent complex, and radical-directed dissociation of the peptide yielding backbone and side chain fragmentation.²⁹

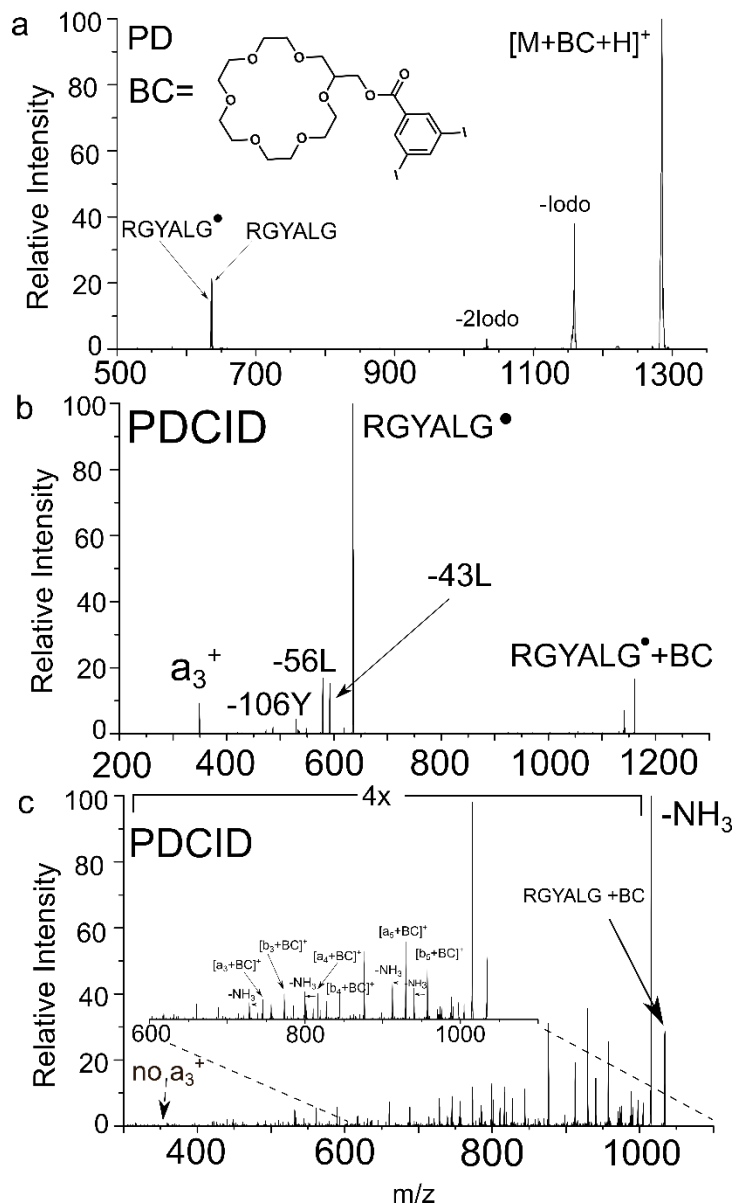
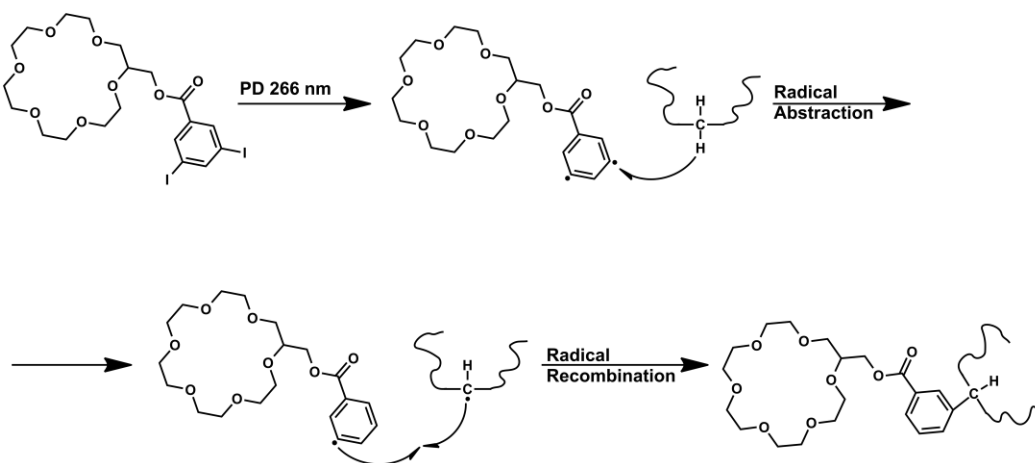


Figure 4: a) PD of the peptide RGYALG complexed with BC. Subsequent CID on either the b) single iodine loss or c) double iodine loss is shown. Peptide fragments indicate BC is attached near the N-terminus of the peptide.

The second most abundant products in Fig. 4a are protonated RGYALG in both radical and canonical form, but there is also a minor product corresponding to the loss of two iodine atoms. This product would correspond to the diradical shown in Scheme 2. Aromatic radicals are highly

reactive and capable of abstracting hydrogen from most sites with a peptide.³⁰ Abstraction of hydrogen, as shown in Scheme 2, would result in net migration of the radical from the BC to the peptide, a process already confirmed to occur in both Figures 4a and 4b. If the remaining radical then reorients via rotation, it could recombine with the radical site on the peptide and form a new covalent bond. Collisional activation of the two iodine loss peak yields the spectrum shown in Fig. 4c, which is dominated by various backbone fragments. Importantly, the loss of BC is not observed, consistent with covalent bond formation. Furthermore, the observation of a_3 ions with BC attached, and absence of a_3 ions without BC suggests attachment near the N-terminus. Given that the BC must be attached to either the side chain of arginine or the N-terminal amine,³¹⁻³³ this result suggests that localized cross-linking was favored.



Scheme 2: Radical recombination of BC with peptide following photoactivation at 266 nm.

To explore the potential for using BC to identify crown ether binding sites, experiments were conducted with melittin (GIGAVLKVL TGLPALISWI KRKRQQ-NH₂), which contains lysine residues near the N- and C-termini. Figure 5a and 5b show results from collisional activation of the double iodine losses for the 3+ and 4+ charge states of melittin+BC noncovalent complexes. The most probable sites of crown ether attachment are highlighted in red on the peptide

sequence in Fig. 5b. The most abundant fragment for both the 3+ and 4+ charge states is the loss of the BC without recombination, but a significant number of backbone fragments with BC attached are also observed. Analysis of the fragment ions from the 3+ charge state indicates the site of modification is near the C-terminus, i.e. y_{13}^{2+} y_{17}^{2+} y_{18}^{2+} y_{19}^{2+} and y_{20}^{2+} ions all have BC attached while the a_9^{2+} does not. A similar conclusion is drawn from the series of b and y-ions identified for the +4-charge state (although the exact fragment ions differ). These results suggest that the binding site rich KRKR sequence near the C-terminus of melittin is the preferred binding site.

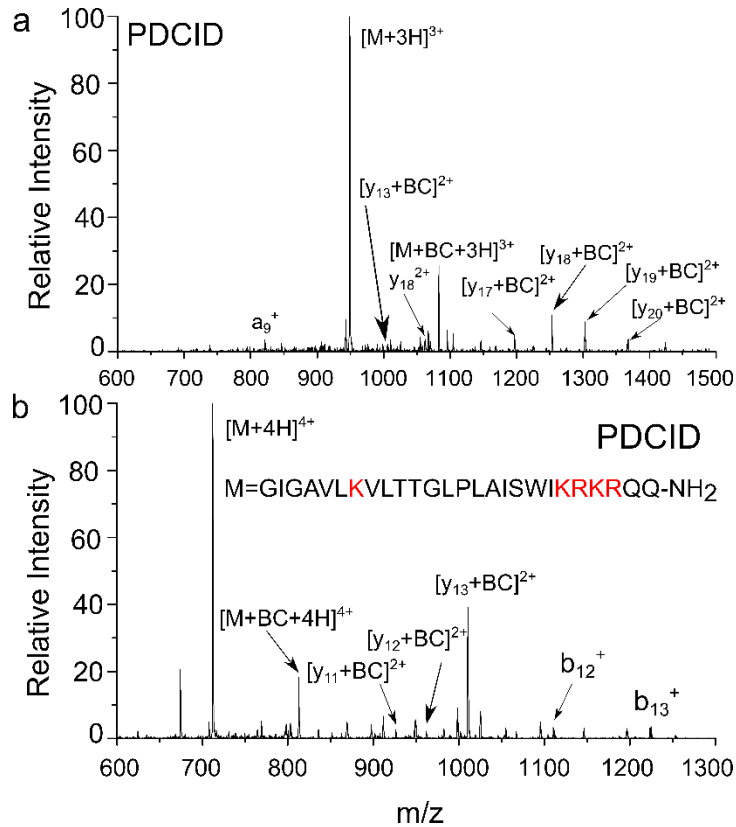


Figure 5: PDCID of the a) +3 and b) +4 charge states of the small protein melittin (GIGAVLKVLT TGLPLAISWIKRKRQQ-NH₂). Possible sites for the noncovalent attachment of BC are labeled in red.

The small protein ubiquitin has been studied extensively by mass spectrometry.³⁴⁻⁴⁰ Investigation of the preferred 18-crown-6 binding sites has been evaluated by site directed mutagenesis where each lysine residue was sequentially removed in a difficult and time-consuming process.⁴¹ For comparison, the preferred binding site was examined herein by electrospraying a mixture of ubiquitin and BC, followed by photoactivation of a single-adduct noncovalent complex, see Fig. 6a. Collisional activation of double iodine-loss peak yields the spectrum shown in Fig. 6b. The most abundant product is loss of the BC adduct, but many b and y ions are also detected. A series of y-ions out to y_{60}^{5+} is observed with no BC attached, consistent with BC being attached near the N-terminus. A single b-ion with BC attached is also detected, although unfortunately, the ion corresponds to b_{58}^{5+} and does not significantly constrain the location of the BC adduct. However, when taken as a whole, the fragments in Fig. 6b suggest that the BC attaches near the N-terminus, in agreement with previous results.⁴¹ These results were obtained in relatively simple experiments and reveal that diradical attack to create covalent crosslinks is a promising way to extract structural information about noncovalent assemblies. To verify the location of noncovalent binding, additional experiments could be conducted where potential sites identified rapidly by BC binding would be mutated to non-interacting residues.

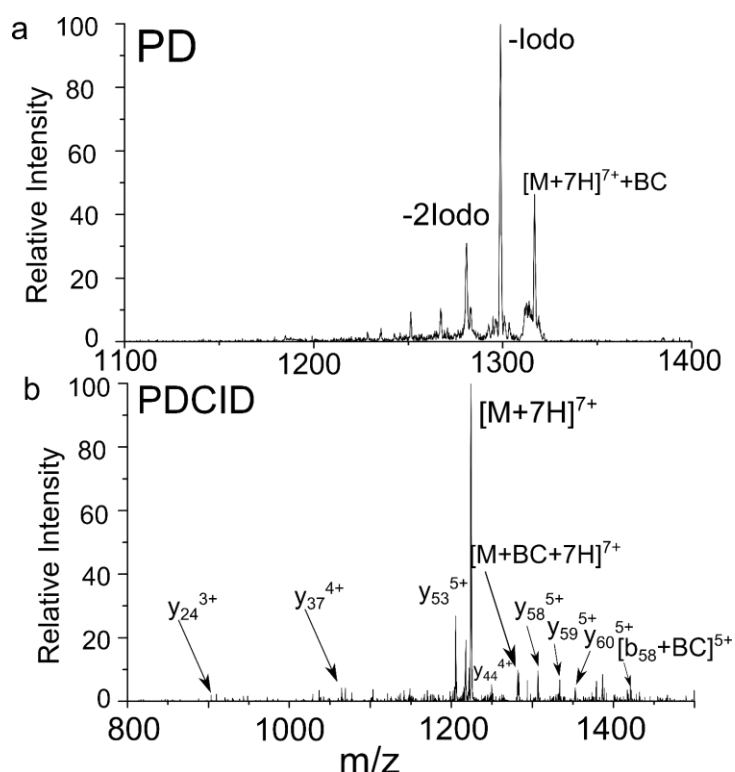


Figure 6: a) PD of the +7 charge state of ubiquitin and BC complex. b) CID on the loss of 2 iodine produces fragment ions which localize modification to the N-terminal side of ubiquitin

Conclusion.

The present results indicate that radicals can be utilized for the formation of new S-S and C-C bonds in the gas phase. Interestingly, in one case unreactive sulfur radicals are used, while in the other highly reactive aromatic phenyl radicals form new bonds. In both situations, the relative reactivity is key for successful creation of a new bond. Disulfide bonds can be formed through the photoactivation of peptide species containing two PM modified cysteines. Simultaneous or sequential loss of both PM groups leads to the formation of a new disulfide bond. Formation of these new disulfide bonds occurs both intermolecularly and intramolecularly. These observations suggest that thiol radicals are quite selective, preferring to attack other thiol radicals or disulfide bonds while leaving most sites in peptides untouched. In UVPD and ECD experiments where sulfur radicals could be formed, caution should be taken when examining

proteins containing multiple disulfide bonds where gas phase disulfide scrambling could occur even if only a single disulfide bond were homolytically cleaved.

Diradical initiated bond formation is also shown to be useful for identifying sites of interaction for crown ether based noncovalent complexes. The sites of adduction do not appear to be random, but occur at preferred locations. Crown ethers have also been shown to replace solvent in peptides and proteins sprayed into a mass spectrometer,⁴²⁻⁴⁴ helping maintain their liquid phase structure. Diradical covalent coupling may provide useful insights into the sites of solvation that help retain tertiary structure as proteins are transferred from liquid to the gas phase.

Acknowledgements. The authors gratefully acknowledge funding from the NSF (CHE-1401737) and NIH (NIGMS grant R01GM107099).

References

- ¹ Shaffer, C. J.; Andrikopoulos, P. C.; Řezáč, J.; Rulíšek, L.; Tureček, F. "Efficient Covalent Bond Formation in Gas-Phase Peptide–Peptide Ion Complexes with the Photoleucine Stapler" *J. Am. Soc. Mass Spectrom.* **2016**, 27, 633–645.
- ² Julian, R. R.; May, J. A.; Stoltz, B. M.; Beauchamp, J. L. "Molecular mousetraps: Gas-phase studies of the covalent coupling of noncovalent complexes initiated by reactive carbenes formed by controlled activation of diazo precursors" *Angew. Chem. Int. Ed.* **2003**, 42, 1012–1015.
- ³ Han, H.; McLuckey, S. A. "Selective Covalent Bond Formation in Polypeptide Ions via Gas-Phase Ion / Ion Reaction Chemistry" **2009**, 12–13.
- ⁴ Stutzman, J. R.; Hassell, K. M.; McLuckey, S. A. "Dissociation behavior of tryptic and intramolecular disulfide-linked peptide ions modified in the gas phase via ion/ion reactions" *Int. J. Mass Spectrom.* **2012**, 312, 195–200.
- ⁵ McGee, W. M.; Mentinova, M.; McLuckey, S. A. "Gas-Phase Conjugation to Arginine Residues in Polypeptide Ions via N-Hydroxysuccinimide Ester-Based Reagent Ions" *J. Am. Chem. Soc.* **2012**, 134, 11412–11414.
- ⁶ Lee, S.; Julian, R. R.; Valentine, S. J.; Reilly, J. P.; Clemmer, D. E. "Biomolecular condensation via ultraviolet excitation in vacuo" *Int. J. Mass Spectrom.* **2012**, 316–318.
- ⁷ Zhang, X.; Julian, R. R. "Photoinitiated intramolecular diradical cross-linking of polyproline peptides in the gas phase" *Phys. Chem. Chem. Phys.* **2012**, 14, 16243.
- ⁸ Ly, T.; Zhang, X.; Sun, Q.; Moore, B.; Tao, Y.; Julian, R. R. "Rapid, quantitative, and site specific synthesis of biomolecular radicals from a simple photocaged precursor" *Chem. Commun.* **2011**, 47, 2835.
- ⁹ Talbert, L. E.; Julian, R. R. "Directed-Backbone Dissociation Following Bond-Specific Carbon-Sulfur UVPD at 213 nm" *J. Am. Soc. Mass Spectrom.* **2018**, 29, 1760–1767.
- ¹⁰ R. Julian, R. "The Mechanism Behind Top-Down UVPD Experiments: Making Sense of Apparent Contradictions" *J. Am. Soc. Mass Spectrom.* **2017**, 28, 1823–1826.
- ¹¹ Sohn, C. H.; Gao, J.; Thomas, D. A.; Kim, T. Y.; Goddard, W. A.; Beauchamp, J. L. "Mechanisms and energetics of free radical initiated disulfide bond cleavage in model peptides and insulin by mass spectrometry" *Chem. Sci.* **2015**, 6, 4550–4560.
- ¹² Moore, B. N.; Blanksby, S. J.; Julian, R. R. Ion-Molecule Reactions Reveal Facile Radical Migration in Peptides. *Chem. Commun.* **2009**, No. 33, 5015–5017.
- ¹³ Ly, T.; Julian, R. R. Elucidating the Tertiary Structure of Protein Ions in Vacuo with Site Specific Photoinitiated Radical Reactions. *J. Am. Chem. Soc.* **2010**, 132 (25), 8602–8609.
- ¹⁴ Diedrich, J. K.; Julian, R. R. Facile Identification of Phosphorylation Sites in Peptides by Radical Directed Dissociation. *Anal. Chem.* **2011**, 83 (17), 6818–6826.
- ¹⁵ I.K. Chu, J. Laskin, Formation of Peptide Radical Ions through Dissociative Electron Transfer in Ternary Metal–Ligand–Peptide Complexes, *Eur. J. Mass Spectrom.* 17 (2011) 543–556.
- ¹⁶ C.K. Barlow, W.D. McFadyen, R.A.J. O'Hair, Formation of Cationic Peptide Radicals by Gas-Phase Redox Reactions with Trivalent Chromium, Manganese, Iron, and Cobalt Complexes†, *J. Am. Chem. Soc.* 127 (2005) 6109–6115.
- ¹⁷ Lee, M.; Kang, M.; Moon, B.; Oh, H. Bin. Gas-Phase Peptide Sequencing by TEMPO-Mediated Radical Generation. *Analyst* **2009**, 134 (8), 1706–1712.
- ¹⁸ M. V Trivedi, J.S. Laurence, T.J. Siahaan, The role of thiols and disulfides on protein stability, *Curr. Protein Pept. Sci.* 10 (2009) 614–625.
- ¹⁹ S.Y. Huang, S.F. Chen, C.H. Chen, H.W. Huang, W.G. Wu, W.C. Sung, Global Disulfide Bond Profiling for Crude Snake Venom Using Dimethyl Labeling Coupled with Mass Spectrometry and RADAR Algorithm, *Anal. Chem.* 86 (2014) 8742–8750.
- ²⁰ P. Anand, A. Grigoryan, M.H. Bhuiyan, B. Ueberheide, V. Russell, J. Quinoñez, P. Moy, B.T. Chait, S.F. Poget, M. Holford, Sample Limited Characterization of a Novel Disulfide-Rich Venom Peptide Toxin from Terebrid Marine Snail *Terebra variegata*, *PLoS One.* 9 (2014) e94122.
- ²¹ Rajpal, G.; Arvan, P. Disulfide Bond Formation. In *Handbook of Biologically Active Peptides*; Elsevier, 2013; pp 1721–1729.
- ²² Agarwal, A.; Diedrich, J. K.; Julian, R. R. "Direct elucidation of disulfide bond partners using ultraviolet photodissociation mass spectrometry" *Anal. Chem.* **2011**, 83, 6455–6458.

- ²³ Hendricks, N. G.; Lareau, N. M.; Stow, S. M.; McLean, J. A.; Julian, R. R. "Bond-specific dissociation following excitation energy transfer for distance constraint determination in the gas phase." *J. Am. Chem. Soc.* **2014**, *136*, 13363–70.
- ²⁴ Hendricks, N. G.; Julian, R. R. "Leveraging ultraviolet photodissociation and spectroscopy to investigate peptide and protein three-dimensional structure with mass spectrometry" *Analyst* **2016**, *141*, 4534–4540.
- ²⁵ Moore, B. N.; Julian, R. R. Dissociation energies of X-H bonds in amino acids. *Phys. Chem. Chem. Phys.* **2012**, *14*, 3148–54.
- ²⁶ M. Lesslie, S. Osburn, M.J. van Stipdonk, V. Ryzhov, Gas-Phase Tyrosine-to-cysteine Radical Migration in Model Systems, *Eur. J. Mass Spectrom.* **21** (2015) 589–597.
- ²⁷ F. Tureček, M. Polášek, A.J. Frank, M. Sadílek, Transient Hydrogen Atom Adducts to Disulfides. Formation and Energetics, *J. Am. Chem. Soc.* **122** (2000) 2361–2370.
- ²⁸ E.H. Krenske, W.A. Pryor, K.N. Houk, Mechanism of SH₂ Reactions of Disulfides: Frontside vs Backside, Stepwise vs Concerted, *J. Org. Chem.* **74** (2009) 5356–5360.
- ²⁹ Q. Sun, H. Nelson, T. Ly, B.M. Stoltz, R.R. Julian, Side Chain Chemistry Mediates Backbone Fragmentation in Hydrogen Deficient Peptide Radicals, *J. Proteome Res.* **8** (2009) 958–966.
- ³⁰ Blanksby, S. J.; Ellison, G. B. Bond Dissociation Energies of Organic Molecules. *Acc. Chem. Res.* **2003**, *36* (4), 255–263.
- ³¹ R.R. Julian, J.L. Beauchamp, Site specific sequestering and stabilization of charge in peptides by supramolecular adduct formation with 18-crown-6 ether by way of electrospray ionization., *Int. J. Mass Spectrom.* **210–211** (2001) 613–623.
- ³² R.R. Julian, M. Akin, J.A. May, B.M. Stoltz, J.L. Beauchamp, Molecular recognition of arginine in small peptides by supramolecular complexation with dibenzo-30-crown-10 ether, *Int. J. Mass Spectrom.* **220** (2002) 87–96.
- ³³ R.R. Julian, J.L. Beauchamp, The unusually high proton affinity of aza-18-crown-6 ether: implications for the molecular recognition of lysine in peptides by lariat crown ethers, *J. Am. Soc. Mass Spectrom.* **13** (2002) 493–498.
- ³⁴ K. Breuker, H. Oh, D.M. Horn, B.A. Cerda, F.W. McLafferty, Detailed Unfolding and Folding of Gaseous Ubiquitin Ions Characterized by Electron Capture Dissociation, *J. Am. Chem. Soc.* **124** (2002) 6407–6420.
- ³⁵ E.W. Robinson, E.R. Williams, Multidimensional separations of ubiquitin conformers in the gas phase: relating ion cross sections to H/D exchange measurements, *J. Am. Soc. Mass Spectrom.* **16** (2005) 1427–1437.
- ³⁶ J.R. Cannon, K. Martinez-Fonts, S.A. Robotham, A. Matouschek, J.S. Brodbelt, Top-Down 193-nm Ultraviolet Photodissociation Mass Spectrometry for Simultaneous Determination of Polyubiquitin Chain Length and Topology, *Anal. Chem.* **87** (2015) 1812–1820.
- ³⁷ S. Warnke, C. Baldauf, M.T. Bowers, K. Pagel, G. von Helden, Photodissociation of Conformer-Selected Ubiquitin Ions Reveals Site-Specific Cis/Trans Isomerization of Proline Peptide Bonds, *J. Am. Chem. Soc.* **136** (2014).
- ³⁸ G. Wang, R.R. Abzalimov, C.E. Bobst, I.A. Kaltashov, Conformer-specific characterization of nonnative protein states using hydrogen exchange and top-down mass spectrometry, *Proc. Natl. Acad. Sci. U. S. A.* **110** (2013) 20087–20092.
- ³⁹ H. Shi, D.E. Clemmer, Evidence for two new solution states of ubiquitin by IMS-MS analysis, *J. Phys. Chem. B.* **118** (2014) 3498–3506.
- ⁴⁰ G.E. Reid, J. Wu, P.A. Chrisman, J.M. Wells, S.A. McLuckey, Charge-State-Dependent Sequence Analysis of Protonated Ubiquitin Ions via Ion Trap Tandem Mass Spectrometry, *Anal. Chem.* **73** (2001) 3274–3281.
- ⁴¹ Liu, Z. J.; Cheng, S. J.; Gallie, D. R.; Julian, R. R. "Exploring the mechanism of selective noncovalent adduct protein probing mass spectrometry utilizing site-directed mutagenesis to examine ubiquitin" *Anal. Chem.* **2008**, *80*, 3846–3852.
- ⁴² J.G. Bonner, N.G. Hendricks, R.R. Julian, Structural Effects of Solvation by 18-Crown-6 on Gaseous Peptides and TrpCage after Electrospray Ionization, *J. Am. Soc. Mass Spectrom.* **27** (2016) 1661–1669.
- ⁴³ Tao, Y.; Julian, R. R. Investigation of Peptide Microsolvation in the Gas Phase by Radical Directed Dissociation Mass Spectrometry. *Int. J. Mass Spectrom.* **2016**, *409*, 81–86.
- ⁴⁴ Warnke, S.; von Helden, G.; Pagel, K. Protein Structure in the Gas Phase: The Influence of Side-Chain Microsolvation. *J. Am. Chem. Soc.* **2013**, *135* (4), 1177–1180.